



Evolutionarily informed deep learning methods for predicting relative transcript abundance from DNA sequence

Jacob D. Washburn^{a,1}, Maria Katherine Mejia-Guerra^a, Guillaume Ramstein^a, Karl A. Kremling^a, Ravi Valluru^a, Edward S. Buckler^{a,b,2}, and Hai Wang^{c,a,1,2}

^aInstitute for Genomic Diversity, Cornell University, Ithaca, NY 14853; ^bAgricultural Research Service, United States Department of Agriculture, Ithaca, NY 14850; and ^cBiotechnology Research Institute, Chinese Academy of Agricultural Sciences, 100081 Beijing, China

Contributed by Edward S. Buckler, January 31, 2019 (sent for review August 24, 2018; reviewed by Karsten M. Borgwardt, Zachary B. Lippman, and Robert Meeley)

Deep learning methodologies have revolutionized prediction in many fields and show potential to do the same in molecular biology and genetics. However, applying these methods in their current forms ignores evolutionary dependencies within biological systems and can result in false positives and spurious conclusions. We developed two approaches that account for evolutionary relatedness in machine learning models: (i) gene-family-guided splitting and (ii) ortholog contrasts. The first approach accounts for evolution by constraining model training and testing sets to include different gene families. The second approach uses evolutionarily informed comparisons between orthologous genes to both control for and leverage evolutionary divergence during the training process. The two approaches were explored and validated within the context of mRNA expression level prediction and have the area under the ROC curve (auROC) values ranging from 0.75 to 0.94. Model weight inspections showed biologically interpretable patterns, resulting in the hypothesis that the 3' UTR is more important for fine-tuning mRNA abundance levels while the 5' UTR is more important for large-scale changes.

machine learning | convolutional neural networks | regulation | RNA

Machine and deep learning approaches such as Convolutional Neural Networks (CNNs) are largely responsible for a recent paradigm shift in image and natural language processing. These approaches are among the fundamental enablers of modern artificial intelligence advances such as facial recognition, speech recognition, and self-driving vehicles. The same deep learning approaches are beginning to be applied to molecular biology, genetics, agriculture, and medicine (1–7), but evolutionary relationships make properly training and testing models in biology much more challenging than the image or text classification problems mentioned above.

For example, if one wants to predict mRNA levels from DNA promoter regions (as we do here), the standard approach from image recognition problems would be to randomly split genes into training and testing sets (8). However, such a split will likely lead to dependencies between the sets because of shared evolutionary histories between genes (i.e., gene family relatedness, gene duplications, etc.) and may cause model overfitting and false-positive spurious conclusions. Models trained without properly accounting for the constraints imposed by evolutionary history (and perhaps other biological and technical factors specific to the modeling scenario) will likely memorize both the neutral and the functional evolutionary history, rather than learning only the functional elements, leading researchers to incorrect conclusions.

With these challenges in mind, we developed two CNN architectures for predicting mRNA expression levels from DNA promoter and/or terminator regions. These include models that predict the following: (i) if a given gene is highly or lowly expressed and (ii) which of two compared gene orthologs has higher mRNA abundance. The architectures are built around

two methods developed here for properly structuring the model training and testing process to avoid the issues of training-set contamination by evolutionary relatedness. The first training method, which we call “gene-family guided splitting,” uses gene-family relationships to ensure that genes within the same family are not split between the training and testing sets. In this way, the model never sees a gene family in the testing set that it has already seen during the training process (Fig. 1A). The second training method uses what we call “ortholog contrasts” (comparisons between pairs of orthologs) to eliminate evolutionary dependencies (Fig. 1B). In addition to controlling for evolutionary relatedness, this method actually allows evolution to become an asset in the training process by leveraging whole-genome duplication events and/or genetic differences between species, two things that would normally be a hindrance to such models. Using evolutionary relatedness is powerful because it allows one to understand and train on what has survived selection. Considering deeper evolutionary divergence, between species rather than just within species, allows for sampling thousands of years of mutagenesis and selective pressures.

Significance

Machine learning methodologies can be applied readily to biological problems, but standard training and testing methods are not designed to control for evolutionary relatedness or other biological phenomena. In this article, we propose, implement, and test two methods to control for and utilize evolutionary relatedness within a predictive deep learning framework. The methods are tested and applied within the context of predicting mRNA expression levels from whole-genome DNA sequence data and are applicable across biological organisms. Potential use cases for the methods include plant and animal breeding, disease research, gene editing, and others.

Author contributions: J.D.W., M.K.M.-G., G.R., K.A.K., E.S.B., and H.W. designed research; J.D.W., K.A.K., E.S.B., and H.W. performed research; J.D.W. and H.W. contributed new analytic tools; J.D.W., R.V., and H.W. analyzed data; and J.D.W. and H.W. wrote the paper.

Reviewers: K.M.B., ETH Zürich; Z.B.L., Cold Spring Harbor Laboratory; and R.M., Corteva Agriscience.

The authors declare no conflict of interest.

Published under the [PNAS license](#).

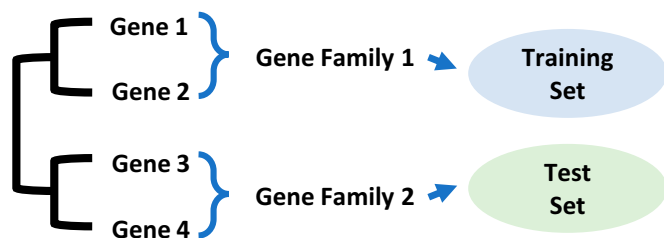
Data deposition: The data reported in this paper has been deposited in the National Center for Biotechnology Information Sequence Read Archive database (accession no. [PRJNA503076](#)) and the Bitbucket repository (https://bitbucket.org/bucklerlab/p_strength_prediction).

¹J.D.W. and H.W. contributed equally to this work.

²To whom correspondence may be addressed. Email: esb33@cornell.edu or wanghai01@caas.cn.

This article contains supporting information online at www.pnas.org/lookup/suppl/doi:10.1073/pnas.1814551116/-DCSupplemental.

A Gene Family Guided Training



B Ortholog Contrast Training

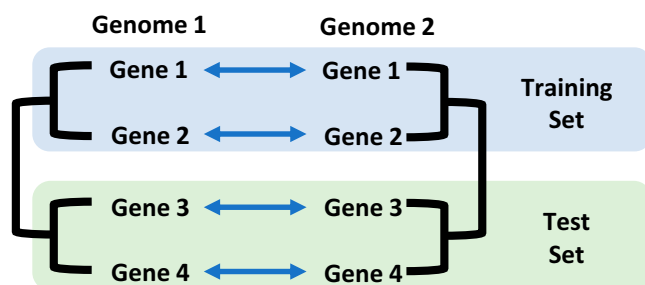


Fig. 1. Evolutionarily informed strategies for deep learning. (A) For prediction tasks involving a single species, genes are grouped into gene families before being further divided into a training and a test set to prevent deep learning models from learning family-specific sequence features that are associated with target variables. (B) For prediction tasks involving two species, orthologs are paired before being divided into a training and a test set to eliminate evolutionary dependencies.

Results

Differentiating Between Expressed and Unexpressed Genes Based on DNA Sequence. The first model was developed for the purpose of classifying genes as being expressed or not expressed (zero or near-zero expression level). This model has been named the “pseudogene model” because of its ability to predict genes that are potentially pseudogenized and therefore lack expression. The pseudogene model also serves as a simple use case for the gene-family-guided splitting approach. It requires as input the promoter and/or terminator sequences (defined in *Materials and Methods* and illustrated in Fig. 2A). To generate the output of the model (i.e., a binary value representing whether a gene is expressed or unexpressed), a comprehensive atlas of gene expression in maize covering major tissues at various developmental stages was generated by applying a unified pipeline on 422 tissues from seven RNA-Seq studies (9–15) (for full details, see *Materials and Methods* and *Datasets S1* and *S2*). The distribution of the maximum log-transformed Transcripts Per Million (logTPM) revealed a peak at the lower tail comprising unexpressed genes (4,562 genes with maximum logTPM ≤ 1) along with normally distributed expressed genes (34,907 genes with maximum logTPM > 1) (Fig. 1B).

As paralogous genes derived from more recent gene duplication events often share highly similar promoters or terminators, overfitting may potentially occur when highly similar paralogs are separated into training and testing sets. Moreover, as paralogs are often similar in their expression levels, separation of highly similar paralogs may force neural networks to learn gene-family-specific sequence features, rather than sequence features that determine expression levels per se. To solve these problems, genes were divided into gene families. The pseudogene model

was trained on randomly selected families and tested on the remaining families not present in the training set (*Dataset S3*).

The number of expressed genes (34,907) and unexpressed genes (4,562) were highly imbalanced. Two approaches were used to handle the imbalance. First, expressed genes were divided into 4,562 highly expressed (maximum TPM ≥ 342.9) genes and 25,783 intermediately expressed genes ($1 < \text{maximum TPM} < 342.9$), and the model was trained to distinguish the 4,562 unexpressed genes from the 4,562 highly expressed genes (Off/High in Fig. 2C). The performance of the pseudogene model was evaluated using a 10 times fivefold cross-validation procedure, and the Off/High version achieved an average predictive accuracy of 86.6% (the area under the ROC curve, auROC = 0.94) when both promoters and terminators were used as the predictor. The average accuracy of the model reached 81.6% (auROC = 0.89) and 80.6% (auROC = 0.89) for promoters and terminators, respectively (Fig. 2C). Second, all expressed genes were randomly down-sampled to make them balanced with unexpressed genes. Using this approach, the model achieved an average predictive accuracy of 74.8% (auROC = 0.82), 70.1% (auROC = 0.77), and 70.6% (auROC = 0.77) for both promoters and terminators, promoters only, and terminators only, respectively (Off/On in Fig. 2C). The models learned higher-level features than single- or dinucleotide composition, since shuffling test set sequences while maintaining single- or dinucleotide composition abolished the predictive accuracy of these models (Fig. 2C) (16).

Random allocation of genes to training/test sets without considering their evolutionary relatedness led to significantly higher performance (in terms of auROC and accuracy) of our models on test-set genes than those obtained by family-guided training/test splitting (*SI Appendix, Fig. S1*). We further categorized the test-set genes into two groups: genes with homologs in the training set and genes without homologs in the training set, and the performance of our models was evaluated on the two groups separately. Interestingly, our models perform significantly more poorly on the latter group than the former group (*SI Appendix, Fig. S1*). Taken together, these results indicate that the evolutionary relatedness between training and test sets, if left uncontrolled, leads to overfitting on gene families present in both training and test sets.

Predicting Which of Two Genes Is More Highly Expressed Using Ortholog Contrasts. The ortholog contrast model follows a simple approach derived from phylogenetics, where the most recent common ancestor of two closely related genes can be represented as a contrast between the two (16, 17). Contrasting genes in this manner directly accounts for statistical dependencies between the genes that would otherwise hamper comparison with other genes (18). Building on this idea, the ortholog contrast method compares two genes from different genomes (or alleles from the same species) to each other and predicts the difference between the expression levels of the two (Fig. 3A). When each gene is compared directly to its ortholog, one can then compare that contrast value to the contrast values from other ortholog pairs without evolutionary dependence between them, hence enabling training and testing sets that are evolutionarily independent (Figs. 1B and 3A). To further simplify the contrast model, the values (the difference between the transcript abundance levels of the two compared genes) were converted to binary form: zero if the first gene is more highly expressed than the second, and 1 in the opposite case. Orthologs with no expression difference between them were excluded. This simplification results in a model where the CNN is asked to determine which of two orthologs is most highly expressed. In reality, this question of deciding between two genes or alleles is actually what is most needed in applications like plant breeding and medicine.

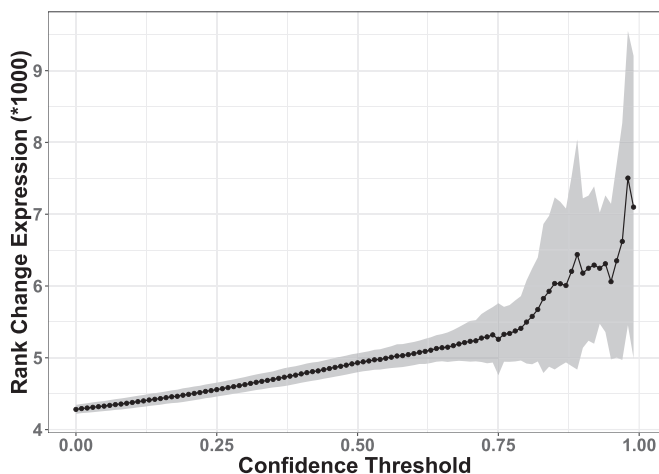


Fig. 4. Model confidence threshold by mean expression rank change between ortholog pairs. A range of model confidence thresholds (model confidence value below which the ortholog pair is excluded from the test set) plotted against the average rank change in expression within each filtered test set across all 10-replicate fivefold validation sets. Pearson correlation coefficient between the values is $r = 0.92$ with a P value < 0.001 .

motifs/putative cis elements, two gradient-based methods [Saliency and DeepLIFT (Deep Learning Important Features)] and one perturbation-based method (Occlusion) (31, 36) were applied to each of the models (Figs. 5 and 6 and *SI Appendix*, Figs. S3 and S4). The maps are based on the average values for all included genes across all 10 times fivefold cross-validations. Interestingly,

the different training methods (gene-family-guided vs. orthologs contrasts) resulted in very different but potentially complementary results as to which regions of the sequence were most important for the prediction task.

In all tested models, the 5' and 3' UTR regions of what we call promoter and terminator sequences were much more important than the regions just outside of the gene models (Figs. 5 and 6). Pseudogene models trained on the off/on data set (Fig. 5*A* and *SI Appendix*, Fig. S3) and off/high data set (Fig. 5*B* and *SI Appendix*, Fig. S3) resulted in similar saliency maps. In both cases, nonpseudogenes showed stronger signals in the promoter regions than in the terminator regions. This is in agreement with the accuracy values for the models shown above (Fig. 2) where predictions based on the promoter sequences alone outperform those based on the terminator sequences alone. These results make sense based on what is currently known about cis regions that are important to gene expression (37).

For models trained using the ortholog contrast method, the results are somewhat different. In this case, the most heavily weighted areas of the input sequences were found in the terminator region (Fig. 6*A* and *SI Appendix*, Fig. S4). This is consistent whether the gene in the first position is more highly expressed than the gene in the second position or vice versa. The greater importance of terminator regions is further shown by the fact that models run with only the terminator sequence perform better than those with only promoter sequences (Fig. 3). The differences between expression values of the compared genes in the contrast model ranged from Log₁₀-transformed TPM values of 0.12–2.80 with an average of 0.66. Log₁₀-transformed TPM values for the off/high gene set in the pseudogene model ranged from 0 to 0.301 (with an average of 0.101) for the “off” gene set

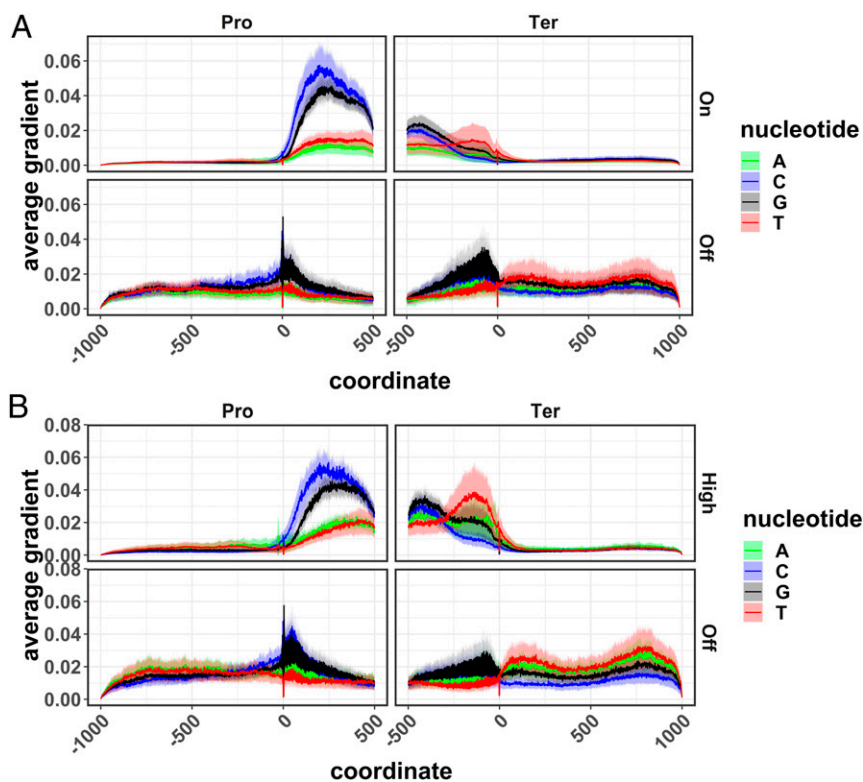


Fig. 5. Averaged saliency map from the pseudogene model. Saliency map was calculated for the pseudogene model trained on either the Off/On gene set (A) or the Off/High gene set (B). Saliency was averaged over nonpseudogenes (Upper) and pseudogenes (Lower), respectively. Only genes with correctly predicted expression levels were used for the calculation of saliency maps. This figure is based on the average values over 10 times fivefold cross-validation, with solid lines representing the mean and shaded areas representing the SD.

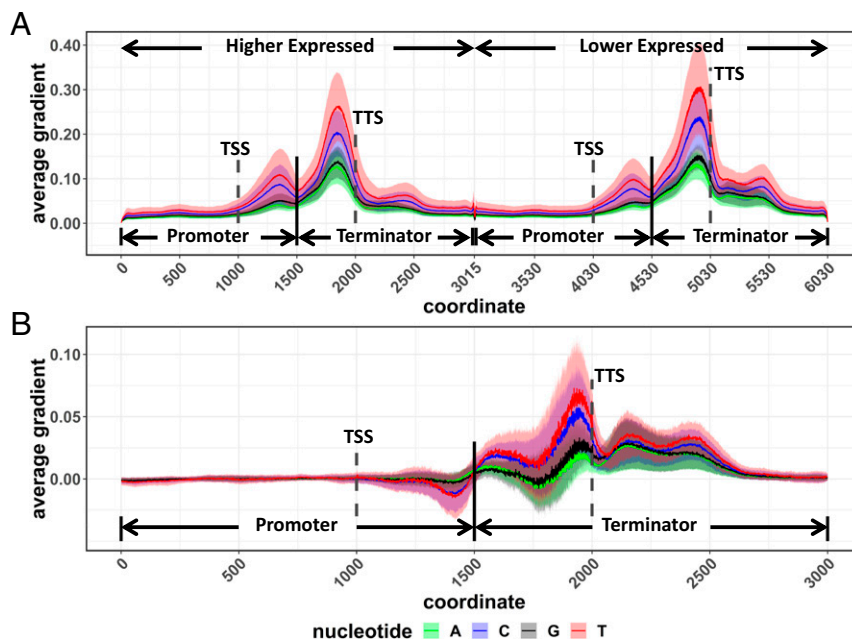


Fig. 6. Averaged saliency maps from the ortholog contrast model. Saliency maps were calculated for the ortholog contrast model. (A) True positive with ortholog 1 more highly expressed than ortholog 2. (B) True positive lower expressed orthologs minus true positive higher expressed orthologs. This figure is based on the average values from all genes over 10 times fivefold cross-validation, with solid lines representing the mean and shaded areas representing the SD.

and ranged from 2.536 to 4.925 (with an average of 2.959) for the “high” gene set.

While pseudogenes (not expressed) in the family-guided approach showed very little signal in the promoter and terminator regions, the lower expressed genes in the contrast model actually showed very strong signals in these regions (at least for the saliency and occlusion methods). In the case of the terminator region, lower expressed genes showed higher values than highly expressed genes (Fig. 6B) for the saliency method, while the promoter regions showed the opposite trend with higher saliency, occlusion, and DeepLIFT values in the more highly expressed gene. All three feature-importance methods indicate that the terminator region is more important than the promoter region in the contrast model, giving us high confidence in this conclusion. Conversely, one of the three methods (saliency) shows higher values for the lower expressed gene, although these values are within one SD of the mean. The other two methods show similar values for both high and low (occlusion) or the opposite trend with higher expressed genes having higher values and lower expressed genes having very low values (DeepLIFT). This result is inconsistent across the three methods, making it harder to interpret with confidence.

Discussion

3' UTR Potentially More Important for Small-Scale Changes in RNA Abundance. There are a number of factors that might explain the differences in promoter and terminator importance between the pseudogene and ortholog contrast models. First, the method of controlling for evolutionary relatedness differs between the models. The grouping of genes into families for the gene-family-guided method relies on sequence similarity scores with subjectively defined cutoffs. This method is therefore potentially over- or under-controlling (or both in the case of different genes) for evolutionary relationships. The ortholog contrast model, on the other hand, fully controls for these relationships. Second, the pseudogene model is restricted to a single species while the contrast was applied both within species (although between subgenomes) and across species. Finally, and perhaps most likely, is that the two models are focused on different categories

of gene expression and genes that have experienced different types of evolutionary constraint. The pseudogene model includes a bimodal distribution of genes that are expressed (highly or moderately) and genes that are not expressed, while the contrast model mostly contains genes that are expressed at some level (that likely does not include many pseudogenes). Given that small mutations in the promoter region could conceivably inhibit protein:DNA interactions and be responsible for drastic changes in gene expression (such as turning expression on or off), perhaps these types of mutations are responsible for the high predictive importance of promoter regions in the pseudogene model. The contrast model, on the other hand, was limited to genes with matching single-copy syntenic orthologs between distinct genomes to ensure reliable normalization and a balanced dataset for training and testing. These genes will be highly conserved (by definition) and likely under strong purifying selection to have remained conserved since the maize/sorghum split, meaning that large-scale expression changes are unlikely to be tolerated. Small-scale, fine-tuning adjustments of expression level, on the other hand, are more likely to be present in these highly conserved genes. We therefore hypothesize that the terminator region (particularly the 3' UTR) plays a more important role in small-scale fine-tuning of RNA abundance levels than does the promoter (particularly the 5' UTR) region. While the promoter and 5' UTR regions are often thought of as important to transcriptional regulation, it has been known for some time that the 3' UTR also plays an important role (38, 39). The 3' UTR has been shown to regulate transcription via diverse mechanisms such as alternative polyadenylation, riboswitching, Nonsense-mediated decay, and alternative splicing (37). Which of these or other possible mechanisms may be at play here is not obvious, but the results presented here strongly implicate the 3'-UTR region in determining expression differences between syntenic orthologs across genomes.

Strengths and Weaknesses of Different Models and Training Approaches. We have demonstrated the utility of two different approaches for mRNA expression prediction. Both approaches incorporate methods for dealing with evolutionary relatedness

were then concatenated together with a block of all zero columns equivalent to 30 bp in between them. Different lengths of padding between the two sequences were tried, but 30 bp worked well and was used for all reported analyses. To control for the possibility of the network learning gene order (i.e., the first gene is always more highly expressed than the second), all gene pairs were fed to the model in both possible orders.

Transcript abundance data used in the contrast model included only one tissue type (shoot tissue) based on at least two replicates (distinct libraries created from pooled plants) for both maize and sorghum as described in ref. 46. Fragment Per Million values were log₂-scaled and then normalized by percentage rank based only on genes with single-copy syntenic orthologs in both genomes. In cases where multiple transcripts had the same expression

values, the average rank value was assigned to all. Orthologs were then paired and filtered to exclude pairs with a less than 2,000 rank expression difference between them ($\sim 0.12 \log_{10}$ TPM) and down-sampled to ensure an equal number of sorghum and maize winners. This resulted in 3,094 ortholog pairs for use in model training, validation, and testing.

ACKNOWLEDGMENTS. We thank James Schnable for maize and sorghum ortholog lists. This material is based upon work supported by the NSF Postdoctoral Research Fellowship in Biology under Grant 1710618 (to J.D.W.); the NSF Plant Genome Research Program under Grant 1238014 (to E.S.B.); and the Tang Cornell-China Scholars Program (H.W.). Additional support comes from the United States Department of Agriculture, Agricultural Research Service.

- Quang D, Xie X (2017) FactorNet: A deep learning framework for predicting cell type specific transcription factor binding from nucleotide-resolution sequential data. *bioRxiv*, 10.1101/151274.
- Alipanahi B, Delong A, Weirauch MT, Frey BJ (2015) Predicting the sequence specificities of DNA- and RNA-binding proteins by deep learning. *Nat Biotechnol* 33: 831–838.
- Ching T, et al. (2018) Opportunities and obstacles for deep learning in biology and medicine. *J R Soc Interface* 15:pii: 20170387.
- Demirci S, Peters SA, de Ridder D, van Dijk ADJ (2018) DNA sequence and shape are predictive for meiotic crossovers throughout the plant kingdom. *Plant J*, 10.1111/tj.13979.
- Webb S (2018) Deep learning for biology. *Nature* 554:555–557.
- Leung MKK, Delong A, Alipanahi B, Frey BJ (2016) Machine learning in genomic medicine: A review of computational problems and data sets. *Proc IEEE* 104:176–197.
- Wainberg M, Merico D, Delong A, Frey BJ (2018) Deep learning in biomedicine. *Nat Biotechnol* 36:829–838.
- Chen Y, Li Y, Narayan R, Subramanian A, Xie X (2016) Gene expression inference with deep learning. *Bioinformatics* 32:1832–1839.
- Li P, et al. (2010) The developmental dynamics of the maize leaf transcriptome. *Nat Genet* 42:1060–1067.
- Davidson RM, et al. (2011) Utility of RNA sequencing for analysis of maize reproductive transcriptomes. *Plant Genome J* 4:191–203.
- Chettoor AM, et al. (2014) Discovery of novel transcripts and gametophytic functions via RNA-seq analysis of maize gametophytic transcriptomes. *Genome Biol* 15:414.
- Stelpflug SC, et al. (2016) An expanded maize gene expression atlas based on RNA sequencing and its use to explore root development. *Plant Genome*, 10.3835/plantgenome2015.04.0025.
- Bolduc N, et al. (2012) Unraveling the KNOTTED1 regulatory network in maize meristems. *Genes Dev* 26:1685–1690.
- Zhang Y, et al. (2017) Differentially regulated orthologs in sorghum and the subgenomes of maize. *Plant Cell* 29:1938–1951.
- Johnston R, et al. (2014) Transcriptomic analyses indicate that maize ligule development recapitulates gene expression patterns that occur during lateral organ initiation. *Plant Cell* 26:4718–4732.
- Washburn JD, Wang H (2019) Data from "P_strength_prediction." Bitbucket. Available at https://bitbucket.org/bucklerlab/p_strength_prediction/. Deposited July 6, 2018.
- Washburn JD, Kremling KA, Valluru R, Buckler ES, Wang H (2019) Evolutionarily informed deep learning methods: Predicting relative transcript abundance from DNA sequence. National Center for Biotechnology Information: Sequence Read Archive. Available at www.ncbi.nlm.nih.gov/bioproject/PRJNA503076. Deposited October 30, 2018.
- Felsenstein J (1985) Phylogenies and the comparative method. *Am Nat* 125:1–15.
- Ketkar N (2017) *Deep Learning with Python: A Hands-On Introduction* (Apress, New York).
- Esteve A, et al. (2017) Dermatologist-level classification of skin cancer with deep neural networks. *Nature* 542:115–118.
- Hughes TE, Langdale JA, Kelly S (2014) The impact of widespread regulatory neofunctionalization on homeolog gene evolution following whole-genome duplication in maize. *Genome Res* 24:1348–1355.
- Schnable JC, Freeling M (2012) Maize (*Zea mays*) as a model for studying the impact of gene and regulatory sequence loss following whole-genome duplication. *Polyploidy and Genome Evolution* (Springer, Berlin), pp 137–145.
- Lu Z, Ricci WA, Schmitz RJ, Zhang X (2018) Identification of cis-regulatory elements by chromatin structure. *Curr Opin Plant Biol* 42:90–94.
- Core LJ, Waterfall JJ, Lis JT (2008) Nascent RNA sequencing reveals widespread pausing and divergent initiation at human promoters. *Science* 322:1845–1848.
- Kwak H, Fuda NJ, Core LJ, Lis JT (2013) Precise maps of RNA polymerase reveal how promoters direct initiation and pausing. *Science* 339:950–953.
- Lugowski A, Nicholson B, Rissland OS (2018) DRUID: A pipeline for transcriptome-wide measurements of mRNA stability. *RNA* 24:623–632.
- Lugowski A, Nicholson B, Rissland OS (2018) Determining mRNA half-lives on a transcriptome-wide scale. *Methods* 137:90–98.
- Yuh CH, Bolouri H, Davidson EH (1998) Genomic cis-regulatory logic: Experimental and computational analysis of a sea urchin gene. *Science* 279:1896–1902.
- Garneau NL, Wilusz J, Wilusz CJ (2007) The highways and byways of mRNA decay. *Nat Rev Mol Cell Biol* 8:113–126.
- Zhou J, Troyanskaya OG (2015) Predicting effects of noncoding variants with deep learning-based sequence model. *Nat Methods* 12:931–934.
- Shrikumar A, Greenside P, Kundaje A (2017) Learning important features through propagating activation differences. *Proceedings of the 34th International Conference on Machine Learning, Proceedings of Machine Learning Research*, eds Precup D, Teh YW (PMLR, International Convention Centre, Sydney), pp 3145–3153.
- Zintgraf LM, Cohen TS, Adel T, Welling M (2017) Visualizing deep neural network decisions: Prediction difference analysis. *arXiv*, 1702.04595.
- Doshi-Velez F, Kim B (2017) Towards a rigorous science of interpretable machine learning. *arXiv*, 1702.08608.
- Choromanska A, Henaff M, Mathieu M, Ben Arous G, LeCun Y (2014) The loss surfaces of multilayer networks. *arXiv*, 1412.0233.
- Dinh L, Pascanu R, Bengio S, Bengio Y (2017) Sharp minima can generalize for deep nets. *Proceedings of the 34th International Conference on Machine Learning, Proceedings of Machine Learning Research*, eds Precup D, Teh YW (PMLR, International Convention Centre, Sydney), pp 1019–1028.
- Simonyan K, Vedaldi A, Zisserman A (2013) Deep inside convolutional networks: Visualising image classification models and saliency maps. *arXiv*, 1312.6034.
- Srivastava AK, Lu Y, Zinta G, Lang Z, Zhu J-K (2018) UTR-dependent control of gene expression in plants. *Trends Plant Sci* 23:248–259.
- Proudfoot N (2004) New perspectives on connecting messenger RNA 3' end formation to transcription. *Curr Opin Cell Biol* 16:272–278.
- Hunt AG (2008) Messenger RNA 3' end formation in plants. *Curr Top Microbiol Immunol* 326:151–177.
- Schnable PS, et al. (2009) The B73 maize genome: Complexity, diversity, and dynamics. *Science* 326:1112–1115.
- Wei F, et al. (2009) The physical and genetic framework of the maize B73 genome. *PLoS Genet* 5:e1000715.
- Jiao Y, et al. (2017) Improved maize reference genome with single-molecule technologies. *Nature* 546:524–527.
- McCormick RF, et al. (2018) The Sorghum bicolor reference genome: Improved assembly, gene annotations, a transcriptome atlas, and signatures of genome organization. *Plant J* 93:338–354.
- Kim D, Langmead B, Salzberg SL (2015) HISAT: A fast spliced aligner with low memory requirements. *Nat Methods* 12:357–360.
- Pertea M, et al. (2015) StringTie enables improved reconstruction of a transcriptome from RNA-seq reads. *Nat Biotechnol* 33:290–295.
- Kremling KAG, et al. (2018) Dysregulation of expression correlates with rare-allele burden and fitness loss in maize. *Nature* 555:520–523.
- Enright AJ, Van Dongen S, Ouzounis CA (2002) An efficient algorithm for large-scale detection of protein families. *Nucleic Acids Res* 30:1575–1584.